Supplement of Atmos. Chem. Phys., 25, 13007–13018, 2025
https://doi.org/10.5194/acp-25-13007-2025-supplement

Atmospheric Chemistry and Physics
Open Access

Supplement of

Different response characteristics of ambient hazardous trace metals and health impacts to global emission reduction

Wenwen Sun et al.

Correspondence to: Rui Li (rli@geo.ecnu.edu.cn)

S1. The development of anthropogenic trace metal emission inventory.

This study quantifies global anthropogenic atmospheric emissions of nine high-toxicity trace metals (As, Cd, Cr, Cu, Mn, Ni, Pb, V, and Zn) by integrating dynamic emission factors with activity levels across source categories. Seven major sources including coal combustion, liquid fuel combustion, ferrous metal smelting, nonferrous metal smelting, non-metallic minerals manufacturing, municipal solid waste incineration, and brake wear were classified. The calculation methodologies for different source sectors are summarized as follows:

$$E(t)=\sum_i\sum_j\sum_k[A_{i,j,k}(t)\times C_{i,j,k}(t)\times R_{i,j}\times(1-\eta_{PM})(1-\eta_{SO_2})(1-\eta_{NOx})\quad \text{(S1)}$$

$$E(t)=\sum_i(F\times C_{Pb}\times A_i)\quad \text{(S2)}$$

$$E(t)=\sum_i\sum_m\sum_n(N_{i,m}\times M_m\times EF_{EF}^{TSP}\times C_n^{v})\quad \text{(S3)}$$

$$E(t)=\sum_i\sum_j[A_{i,j}(t)\times EF_j^{nc}(t)]\quad \text{(S4)}$$

where (S1), (S2), (S3) and (S4) represent the calculation equations for coal combustion by power plants, industrial sectors and other sectors, Pb emission from vehicle gasoline combustion, brake wear, and coal combustion by residential sectors and non-coal combustion sources power plants, respectively. where E(t) is the anthropogenic atmospheric emissions of As, Cd, Cr, Cu, Mn, Ni, Pb, V, and Zn; EF^c and EF^{nc} denote the emission factors for coal combustion and non-coal combustion sources in calendar year t, respectively; A represents the annual activity level, while C is the average concentration of each trace metal in coal; R indicates the fraction of trace metals released into flue gas from coal combustion facilities; η_{PM}, η_{SO2}, and η_{NOx} represent the average removal efficiencies of trace metals by conventional $PM/SO_2/NO_x$ emission control devices, respectively; F represents the proportion of lead in gasoline emitted to the atmosphere. C_{Pb} is the average content of Pb in the gasoline; N denotes the vehicle population; M is the average annual mileage driven by vehicle in category m (passenger car, bus and coach, light-duty truck, and heavy-duty vehicle); EF^{TSP} is the emission factor of total suspended particles (TSP) for brake pad by vehicle category m.

All of the countries are classified into five clusters and each cluster possessed different EF by source categories. The detailed emission factors used in our study were collected from Zhu et al. (2020). The detailed emission factors from multiple sources have been introduced in the following tables. The total emission was allocated to the grid based on the high-resolution population data.

The temporal allocation of trace metal emissions was performed based on the Hg emission inventory developed by Emission Database for Global Atmospheric Research (EDGAR). At last, the monthly anthropogenic trace metal emission inventories at 0.5° spatial resolution were established.

Table S1 Regional definitions for different countries considered in this study.

Continent	Region	Country
Asia	1	Japan
	2	Hong Kong, Israel, South Korea, Singapore, Taiwan
	3	China
	4	Brunei, India, Kazakhstan, Malaysia, Mongolia, Pakistan, Philippines, Sri Lanka, Turkey, Azerbaijan, Iran, Indonesia, Saudi Arabia, Uzbekistan, Oman, Thailand, North Korea, Viet Nam, Tajikistan, Kyrgyzstan, Armenia, Bahrain, Lebanon, Syria, Georgia, Jordan, Qatar, United Arab Emirates, Iraq, Kuwait, Turkmenistan, Maldives, Palestine
	5	Bangladesh, Myanmar, Laos, Afghanistan, Bhutan, Nepal, Yemen, Cambodia
North America	1	US
	2	Canada
	4	Mexico, Trinidad and Tobago, Costa Rica, El Salvador, Nicaragua, Panama, Honduras, Guatemala
	5	Haiti
South America	4	Brazil, Chile, Argentina, Colombia, Cuba, Ecuador, Venezuela, Peru, Bolivia, Dominica, Jamaica, Paraguay, Puerto Rico, Uruguay, Suriname, Barbados, Guyana
Europe	1	France, Germany, Italy, Netherlands, Spain, United Kingdom, Austria, Belgium, Switzerland, Sweden, Portugal, Norway, Iceland, Luxembourg, Ireland, Greece, Finland, Denmark
	2	Czech Republic, Slovenia, Estonia, Slovakia, Hungary, Cyprus, Latvia
	4	Belarus, Russia, Ukraine, Poland, Albania, Bosnia and Herzegovina, Croatia, Romania, Bulgaria, Macedonia, Montenegro, Serbia, Lithuania, Moldova, Kosovo
Africa	4	South Africa, Algeria, Ghana, Egypt, Zimbabwe, Nigeria, Morocco, Kenya, Zambia, Namibia, Botswana, Mauritius, Swaziland, Tunisia, Angola, Libya, Cameroon, Gabon, Lesotho, Côte d'Ivoire, Republic of the Congo
	5	Democratic Republic of the Congo, Madagascar, Malawi, Mozambique, Niger, Senegal, Tanzania, Mauritania, Uganda, Benin, Burkina Faso, Ethiopia, Guinea, Rwanda, Sierra Leone, Sudan, Togo, Burundi Gambia, Mali, Somalia, Chad, Liberia
Oceania	2	Australia New Zealand
	4	Fiji, New Caledonia

Table S2 The emission factors (Unit: g/t) of nine trace metals from coal combustion source in five regions of the world.

Coal-fired power plant		As	Pb	Cd	Cr	Ni	Mn	V	Cu	Zn
	s	4.5	4.5	4.5	4.5	4.5	4.5	4.5	4.5	4.5
Region 1	1995	0.15	0.65	0.02	0.47	0.30	0.22	0.25	0.36	0.24
	2012	0.02	0.07	0.00	0.03	0.04	0.04	0.05	0.04	0.12
	s	5.5	5.5	5.5	5.5	5.5	5.5	5.5	5.5	5.5
Region 2	1995	0.29	1.30	0.03	0.94	0.59	0.44	0.32	0.73	0.50
	2012	0.04	0.12	0.00	0.27	0.18	0.14	0.08	0.22	0.18
Region 3	1995	0.58	1.50	0.05	1.19	1.02	3.01	2.60	1.04	3.00
	2012	0.18	0.39	0.01	0.28	0.26	1.53	0.99	0.77	1.18
	s	4	4	4	4	4	4	4	4	4
Region 4	1995	1.04	5.52	0.10	4.74	0.95	5.38	4.96	2.38	4.72
	2012	0.54	1.07	0.03	0.86	0.70	3.08	2.85	1.37	2.33
	s	4.5	4.5	4.5	4.5	4.5	4.5	4.5	4.5	4.5
Region 5	1995	1.35	5.76	0.12	5.00	1.10	8.53	7.59	3.47	6.98
	2012	1.04	5.52	0.10	4.74	0.95	5.38	4.87	2.38	4.72
Other coal-fired sector		**As**	**Pb**	**Cd**	**Cr**	**Ni**	**Mn**	**V**	**Cu**	**Zn**
	s	/	/	/	/	/	/	/	/	/
Region 1	1995	0.19	1.05	0.02	0.12	0.13	0.22	0.19	0.36	0.24
	2012	0.19	1.05	0.02	0.12	0.13	0.22	0.19	0.36	0.24
	s	4	4	4	4	4	4	4	4	4
Region 2	1995	0.37	2.43	0.05	1.70	0.89	1.50	1.26	1.09	1.50
	2012	0.19	1.05	0.02	0.12	0.13	0.22	0.20	0.36	0.24
Region 3	1995	1.35	5.76	0.12	5.00	1.10	8.53	7.89	3.47	6.98
	2012	1.04	5.52	0.10	4.74	0.95	5.38	4.26	2.38	4.72
	s	4.5	4.5	4.5	4.5	4.5	4.5	4.5	4.5	4.5
Region 4	1995	1.71	6.49	0.14	5.46	1.29	9.56	8.23	4.00	7.66
	2012	1.35	5.87	0.13	4.95	1.12	6.69	7.05	3.47	5.52
	s	4.5	4.5	4.5	4.5	4.5	4.5	4.5	4.5	4.5
Region 5	1995	1.71	6.49	0.14	5.46	1.29	9.56	8.26	4.00	7.66
	2012	1.35	5.87	0.13	4.95	1.12	6.69	5.87	3.47	5.52

Table S3 Emission factors (g/t) of nine trace metals from primary copper smelting industry (EC, 2001b; EEA, 2009, 2013; Nriagu, 1979; Nriagu and Pacyna, 1988; Pacyna, 1984; Pacyna et al., 2002; Pacyna and Pacyna, 2001; Skeaff and Dubreuil, 1997; Streets et al., 2011; Theloke et al., 2008; Tian et al., 2012a, b, c).

Primary Cu smelting		As	Pb	Cd	Cr	Ni	Mn	V	Cu	Zn
Region 1	s	22	22	22	22	22	22	22	22	22
	2012	30	70	2.8	0.05	10	0.5	0.5	90	100
Region 2	s	27	27	27	27	27	27	27	27	27
	2012	50	100	10	0.1	25	0.8	0.8	138	188
Region 3	s	30	30	30	30	30	30	30	30	30
	2012	100	200	50	1	50	4.5	4	250	300
Region 4	s	40	40	40	40	40	35	35	40	35
	2012	320	810	133	4	775	8	8	1500	360
Region 5	s	45	45	45	45	45	45	45	45	45
	2012	1000	3000	200	20	1500	35	35	2494	1000

Table S4 Emission factors (g/t) of nine trace metals from ferrous metal smelting industry (Nriagu, 1979; Nriagu and Pacyna, 1988; Pacyna, 1984; Kakareka et al., 1998; UK, 2000; EC, 2001a; Theloke et al., 2008; EEA, 2009; Pirrone et al., 2010; Streets et al., 2011; UK, 2013).

Iron smelt industry		As	Pb	Cd	Cr	Ni	Mn	V	Cu	Zn
World	1900	3.500	3.495	1.600	2.667	12.00	0.830	0.76	20.00	57.14
Region 1	s	22	22	22	22	22	22	22	22	22
	2012	0.001	0.0005	0.002	0.0002	0.002	0.070	0.06	0.015	0.073
Region 2	s	27	27	27	27	27	27	27	27	27
	2012	0.010	0.015	0.008	0.001	0.025	0.077	0.045	0.155	2.900
Region 3	s	30	30	30	30	30	30	30	30	30
	2012	0.080	0.070	0.016	0.080	0.120	0.082	0.062	0.400	4.000
Region 4	s	40	40	40	40	40	40	40	40	35
	2012	0.100	0.070	0.016	0.080	0.120	0.082	0.065	0.400	7.000
Region 5	s	45	45	45	45	45	45	45	45	45
	2012	0.240	1.250	0.100	0.267	0.356	0.097	0.083	0.789	7.300
Steel smelt industry		**As**	**Pb**	**Cd**	**Cr**	**Ni**	**Mn**	**V**	**Cu**	**Zn**
World	1900	0.558	74.32	2.467	4.112	3.152	129.3	115.6	5.790	190.0
Region 1	s	22	22	22	22	22	22	22	22	22
	2012	0.001	0.072	0.005	0.005	0.015	0.136	0.11	0.010	1.75
Region 2	s	27	27	27	27	27	27	27	27	27
	2012	0.004	0.706	0.010	0.049	0.020	0.400	0.39	0.015	2.30
Region 3	s	30	30	30	30	30	30	30	30	30
	2012	0.011	1.486	0.025	0.123	0.032	2.016	1.845	0.116	6.05
Region 4	s	40	40	40	40	40	40	40	40	35
	2012	0.012	1.555	0.030	0.127	0.050	2.508	2.186	0.138	6.76
Region 5	s	45	45	45	45	45	45	45	45	45
	2012	0.020	7.000	0.044	0.450	0.070	20.00	20.00	0.386	20.00

Table S5 Emission factors (g/t) of nine trace metals for cement industry in different regions of the world (NPI, 2008; Nriagu and Pacyna, 1988; Passant et al., 2002; Streets et al., 2011; US EPA, 2012).

Categories	Years	As	Pb	Cd	Cr	Ni	Mn	V	Cu	Zn
World	1900	13.94	54.43	2.280	11.79	8.120	55.34	12.56	24.20	57.20
Region 1	s	22	22	22	22	22	22	22	22	22
	2012	0.006	0.038	0.001	0.004	0.004	0.036	0.012	0.000	0.130
Region 2	s	27	27	27	27	25	27	27	27	27
	2012	0.026	0.150	0.008	0.010	0.040	0.054	0.048	0.098	0.150
Region 3	s	25	25	25	25	25	25	25	25	25
	2012	0.070	0.380	0.011	0.051	0.041	0.277	0.126	0.121	0.286
Region 4	s	40	40	40	40	40	40	40	40	35
	2012	0.070	0.382	0.011	0.052	0.041	0.279	0.185	0.122	0.288
Region 5	s	45	45	45	45	45	45	45	45	45
	2012	0.345	1.455	0.057	0.100	0.201	1.372	1.056	0.600	0.629

Table S6 Emission factors (g/t) of nine trace metals for glass industry in different regions of the world (EC, 2001c; EEA, 2000).

Categories	Years	As	Pb	Cd	Cr	Ni	Mn	V	Cu	Zn
Region 1	s	3.5	3.5	3.5	3.5	3.5		3.5	3.5	3.5
	1991	0.100	12.00	0.150	2.400	1.900		1.900	0.600	11.00
	2012	0.100	1.500	0.120	0.200	0.200		0.200	0.005	0.300
Region 2	s	4	4	4	4	4		4	4	4
	1991	0.100	12.00	0.150	2.400	1.900		1.900	0.600	11.00
	2012	0.100	1.700	0.130	0.230	0.490		0.490	0.007	0.370
Region 3	s	5	5	5	5	5		5	5	5
	1995	0.248	24.78	0.372	6.194	4.956		4.956	1.239	24.78
	2012	0.101	10.08	0.151	2.519	2.015		2.015	0.504	10.08
Region 4	s		5	5	5	5		5	5	5
	1995	0.248	24.78	0.372	6.194	4.956		4.956	1.239	24.78
	2012	0.142	14.16	0.212	3.541	2.833		2.833	0.708	14.16
Region 5	1995	0.248	24.78	0.372	6.194	4.956		4.956	1.239	24.78
	2012	0.248	24.78	0.372	6.194	4.956		4.956	1.239	24.78

Table S7 Emission factors (g/t) of nine trace metals for brick industry in different regions of the world (NPI, 1998; US EPA, 1996b).

Categories	Years	As	Pb	Cd	Cr	Ni	Mn	V	Cu	Zn
Region 1	1995	0.060	0.069	0.007	0.024	0.033	0.134			
	2012	0.060	0.069	0.007	0.024	0.033	0.134			
Region 2	1995	0.060	0.069	0.007	0.024	0.033	0.134			
	2012	0.060	0.069	0.007	0.024	0.033	0.134			
Region 3	s	5	5	5	5	5	5			
	1995	0.176	0.203	0.020	0.069	0.097	0.392			
	2012	0.060	0.069	0.007	0.024	0.033	0.134			
Region 4	s	5	5	5	5	5	5			
	1995	0.176	0.203	0.020	0.069	0.097	0.392			
	2012	0.092	0.106	0.011	0.036	0.051	0.206			
Region 5	1995	0.176	0.203	0.020	0.069	0.097	0.392			
	2012	0.176	0.203	0.020	0.069	0.097	0.392			

Table S8 Emission factors (g/t) of nine trace metals for MSW incineration in five regions (Nriagu, 1979; Pacyna, 1984; Nriagu and Pacyna, 1988; UK, 2000; US EPA, 1996a, b).

Categories	Years	As	Pb	Cd	Cr	Ni	Mn	V	Cu	Zn
World	1900	2.14	107	5.45	4.49	3.93	9.00	3.96	14.0	60.0
Region 1	s	22	22	22	22	22	22	22	22	22
	2012	0.006	0.058	0.005	0.016	0.022	0.056	0.038	0.014	0.025
Region 2	s	27	27	27	27	27	27	27	27	27
	2012	0.021	0.073	0.007	0.030	0.048	0.131	0.095	0.062	0.097
Region 3	s	30	30	30	30	30	30	30	30	30
	2012	0.053	0.118	0.012	0.037	0.086	0.208	0.125	0.127	0.109
Region 4	s	40	40	40	40	40	40	40	40	35
	2012	0.119	0.219	0.016	0.073	0.134	0.217	0.184	0.278	0.380
Region 5	s	45	45	45	45	45	45	45	45	45
	2012	0.700	0.600	0.124	0.160	0.210	0.392	0.296	0.870	12.50

Table S9 Emission factors (g/t) of nine trace metals from liquid fuel combustion (de Souza et al., 2006; UK, 2013; US EPA, 1996a, c; Wang et al., 2003).

Liquid fuels	As	Pb	Cd	Cr	Ni	Mn	V	Cu	Zn
Crude oil	0.17	0.19	0.05	0.11	10.6	0.22	6.96	0.46	1.04
Fuel oil combustion	0.17	0.19	0.05	0.11	10.6	0.22	6.96	0.46	1.04
Kerosene for stationary sources	0.02	0	0	0	0.06	0.05	0.05	0.03	0.49
Diesel combustion for stationary sources	0.02	0	0	0	0.06	0.05	0.05	0.03	0.49
Gasoline for transportation	0.02	/	0.01	0.01	0.04	0.00	0.04	0.02	0.03
Diesel for transportation	0.02	0.03	0.04	0.04	0.04	0.04	0.04	0.22	0.23
Kerosene for transportation	/	0.06	0.01	0.01	0.03	0	0.04	0.03	0.01

S2. The natural emission inventory of trace metals.

The natural trace metal emissions, including those from soil dust, biomass burning, and sea salt spray, were also estimated in our study. The detailed equations are summarized as follows:

$$W_i(t) = \sum_j \sum_k c_{i,k} \times E_{j,k} \quad \text{(S5)}$$

$$W_i(t) = \sum_{j,k} c_i \times EF_{j,k} \times A_{j,k} \quad \text{(S6)}$$

$$W_i(t) = \sum_{j,k} c_i \times F_j \times V_j \times A_k \times \rho_k \quad \text{(S7)}$$

where (S5), (S6), and (S7) represent the calculation equations for the trace metal emissions from soil dust, biomass burning and sea salt, respectively.

In the equation S5, W(t) represents trace metal emissions from soil dust; c is the average mass concentration of each element in the soil; E represents the dust emissions calculated by the GEOS-Chem model.

In the equation S6, W(t) denotes trace metal emissions from biomass burning; c is the average mass ratio of elements i in terrestrial plants (Table S12); EF is the emission factor of TSP (Table S13). Most of trace metals are released from the particulate matters in combustion processes, and thus particulate matters emissions are applied to estimate emissions of trace metals indirectly; A represents the activity level of biomass burning.

In the equation S7, W_i is emission of element i derived from sea salt aerosol spray; c_i is the average mass concentration for element i in seawater(Conway et al., 2021; Olivelli et al., 2025; Sohrin and Bruland, 2011); F is sea spray flux of radius j; V represents the volume of aerosol particles of radius j; A is sea area, and r denotes seawater density; k refers to different oceans.

Table S10 The trace metal concentrations (Unit: mg/kg) in Asian dust and non-Asian dust.

Species	Asian dust concentration	Non-Asian dust concentration
As	184±139	445±1400
Cd	8.0±6.4	14.1±5.3
Cr	94±42	42±26
Cu	520±958	282±214
Mn	1030±658	1030±658
Ni	172±181	89±58
Pb	1400±1540	1340±911
V	150±85	150±85
Zn	1510±848	1890±491

Table S11 The sensitivity of the global average ratios of soil-derived ambient trace element concentrations and total concentrations (%) to soil trace element concentrations.

	Base	5%	10%	20%	40%
As	35%	35%	36%	38%	42%
Cd	40%	42%	43%	45%	49%
Cr	38%	39%	40%	42%	46%
Cu	33%	34%	35%	37%	41%
Mn	47%	48%	49%	52%	56%
Ni	43%	44%	45%	48%	52%
Pb	40%	41%	42%	44%	48%
V	38%	39%	41%	43%	47%
Zn	40%	42%	43%	45%	49%

Table S12 Average mass ratio of nine trace metals in unit terrestrial plants biomass load.

Trace metals	c (g/t)
As	0.21
Cd	0.18
Cr	0.60
Cu	6.97
Mn	18
Ni	4
Pb	7.6
V	1.25
Zn	13.1

Table S13 Recommended values of fuel load of each unit area for plant cover categories

Plant Cover Categories	**Emission Factor (g PM_{10}/kg Biofuel)**
Warm meadow grassland	5.51
Temperate desert steppe	5.51
Warm desert	5.51
Lowland meadow	5.51
Mountain meadow	5.51
Warm grass	5.51
Hot grass	5.51
Alpine meadow	5.51
Alpine grassland	5.51
temperate steppe	5.51
Cold temperate forest	13.27
Temperate forests	13.27
Warm temperate forest	13.27
North subtropical forest	9.29
Subtropical forest	9.29
South subtropical forest	9.29
Tropical forest	9.29
forest in Tibetan areas	13.27

Table S14 The ground-level observations of nine trace metal concentrations (Unit: ng/m^3) collected from references. In addition, the regular ground-level observations in Europe and North America were obtained from EMEP and EPA websites, respectively.

Site	Country (Macro regions)	Latitude	Longitude	Time	As	Cd	Cr	Cu	Mn	Ni	Pb	V	Zn	References
Baise	China	24°	106.5°	2010.9-10	8.3	1.8	19	7.7			35			Liu et al., 2013
Beijing	China	40°	116.4°	2015.1	16	4	50		105		183		415	(Wu et al., 2019)
Guiyang	China	27°	107°	2009-2010			15	55		20	150		240	(Wang et al., 2011)
Huangshi	China	30.2°	115°	2015	31	3.1	58	47	47	9.9	113	3.9	288	(Hu et al., 2018)
Jiamusi	China	46.8°	130.3°	2024.2		1.9	13	220		7.6	153			
Lanzhou	China	35.6°	103°	2010.7		0.6	19	60		11	99		450	(YU YJ, 2013)
Lanzhou	China	35.6°	103°	2011.1		0.8	20	91		16	220		315	(YU YJ, 2013)
Nanjing	China	32°	118.8°	2014.4-8		3.7	50	49	195	21	103			Zhang et al., 2016
Shijiazhuang	China	38°	114.9°	2016	51	4.1	61	161	158		142	75	345	(Lina et al., 2019)
Tianjin	China	39°	117°	2011	3.1	0.7	34	134		19	487		828	Chen et al., 2013
Weifang	China	36°	119°	2011		2.5	10	60	90	22				Li et al., 2013
Urumqi	China	43°	87°	2007.7-		0.3		279	19		49			(Sun

				8										LongRen et al., 2009)
Wuhan	China	30.5°	114°	2012.10		0.5	6	78	42	2	88			Zhu et al., 2014
Yan'an	China	36°	109°	2018	4	1.2	78				34			Geng et al., 2022
Mexico City	Mexico (NA)	19.4°	-99°	2003-2004		4.2	40		50	6	55	18		(Báez et al., 2007)
Córdoba	Argentina (SA)	-31.6°	-64.2°	2009-2010			8	27	88	6	13	17	64	(López et al., 2011)
Industrial site	Chile (SA)	-23.6°	-70.4°	2007.12	48		4	320	47	3	20	14	83	(Jorquera and Barraza, 2013)
Santiago Island	Cape (SS) Verde	15°	-23.5°	2011			2.6	2.8	31	2.6	2.9		24	(Salvador et al., 2016)
Welgegund	South Africa (SS)	-26.5°	27°	2011	8.4	0.4		6.9	26	79	7.8	37	53	(Venter et al., 2017)

Table S15 Recommended values of the parameters for health risk assessment of trace metals.

Parameter	Adult	Child	Unit
InhR	16.5	8.6	m^3/d
EF	91	91	day
ED	24	6	a
BW	70	15	kg
Cancer AT	91*EF	91*EF	d
Non-cancer AT	ED*EF	ED*EF	d

Table S16 Reference dose (RfD) ($mg\ kg^{-1}\ d^{-1}$) and cancer slope factor (CSF) ($kg\ d\ mg^{-1}$) of selected trace elements in references.

Element	RfD	CSF
As	3×10^{-4}	1.5
Cd	1×10^{-3}	6.3
Cr	3×10^{-3}	5×10^{-1}
Cu	4×10^{-3}	/
Mn	1.4×10^{-5}	/
Ni	2.1×10^{-2}	9×10^{-1}
Pb	2×10^{-2}	5×10^{-1}
V	/	/
Zn	3×10^{-1}	/

Table S17 The contributions (%) of emission change and meteorology to the total changes of health risks. The positive and negative values represented the increased (unfavorable) and decreased (favorable) trace element ratios.

		As	Cd	Cr	Cu	Mn	Ni	Pb	V	Zn
Emission-induced	China	-111	95	-121	-113	-112	129	60	-111	101
	India	-49	-53	-53	-51	-52	-59	-95	-48	-56
	WE	-35	-31	-31	-34	-32	-11	-28	-48	-26
	NA	-114	-103	-109	-111	-114	-113	-138	-107	-100
	SA	-60	-94	-90	-72	-49	-67	-81	-69	-99
	SS	36	-56	-52	23	17	-64	-161	37	-220
	Rus	178	116	94	160	103	34	34	94	228
	Aus	10	63	56	31	-131	70	35	-103	66
Meteo-induced	China	11	5	21	13	12	-29	40	11	-1
	India	-51	-47	-47	-49	-48	-41	-5	-52	-44
	WE	-65	-69	-69	-66	-68	-89	-72	-52	-74
	NA	14	3	9	11	14	13	38	7	0
	SA	-40	-6	-10	-28	-51	-33	-19	-31	-1
	SS	64	156	152	77	83	-36	61	63	320
	Rus	-278	-216	-194	-260	-203	-134	-134	-194	-328
	Aus	90	37	44	69	231	30	65	203	34

Figure S1 The sampling sites of ambient hazardous trace metals at the global scale. The orange dots denote the sampling sites. The colobar reflects the elevation (m).

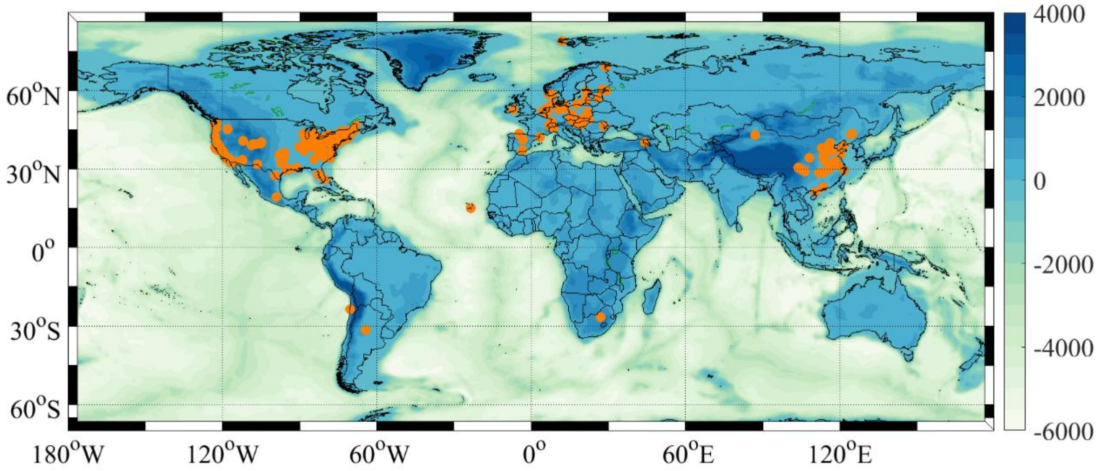

Figure S2 The workflow of the global trace metal emission development and concentration simulation.

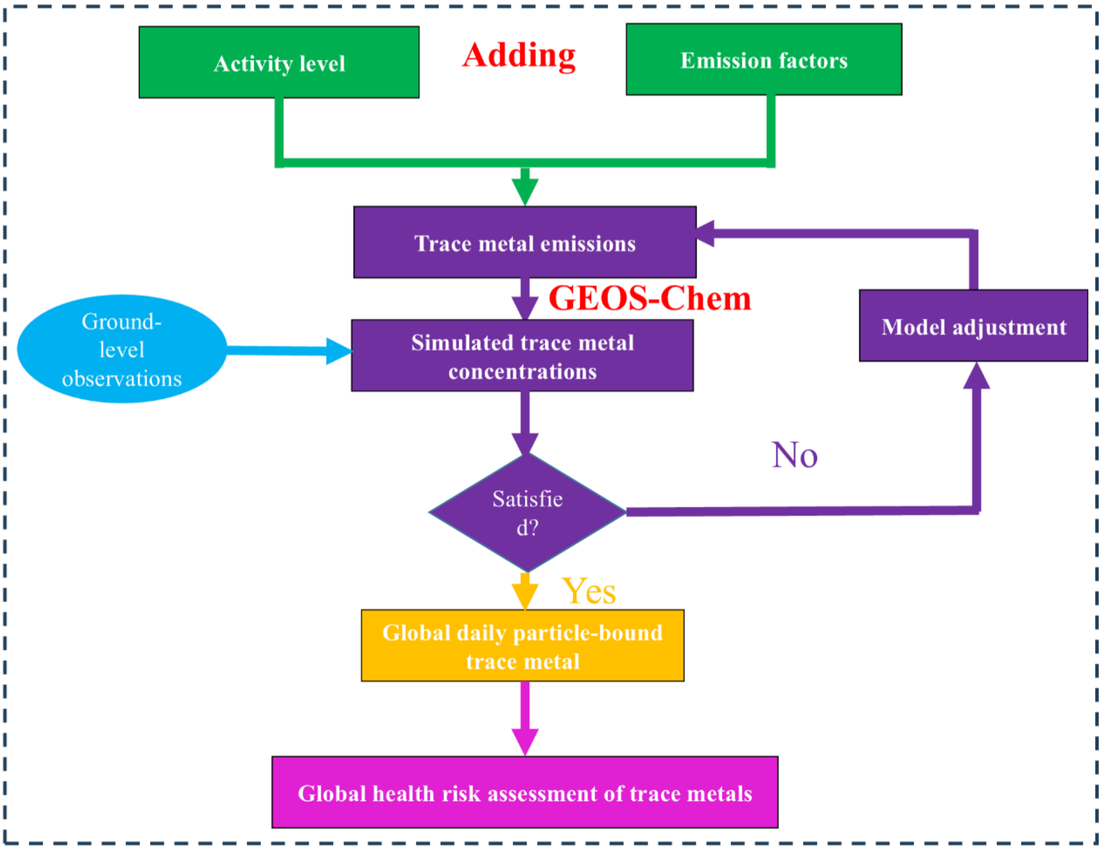

Figure S3 The global variations of ambient trace element concentrations (mean values) during January-April in 2017-2019. The colorbar reflects the concentrations of trace elements.

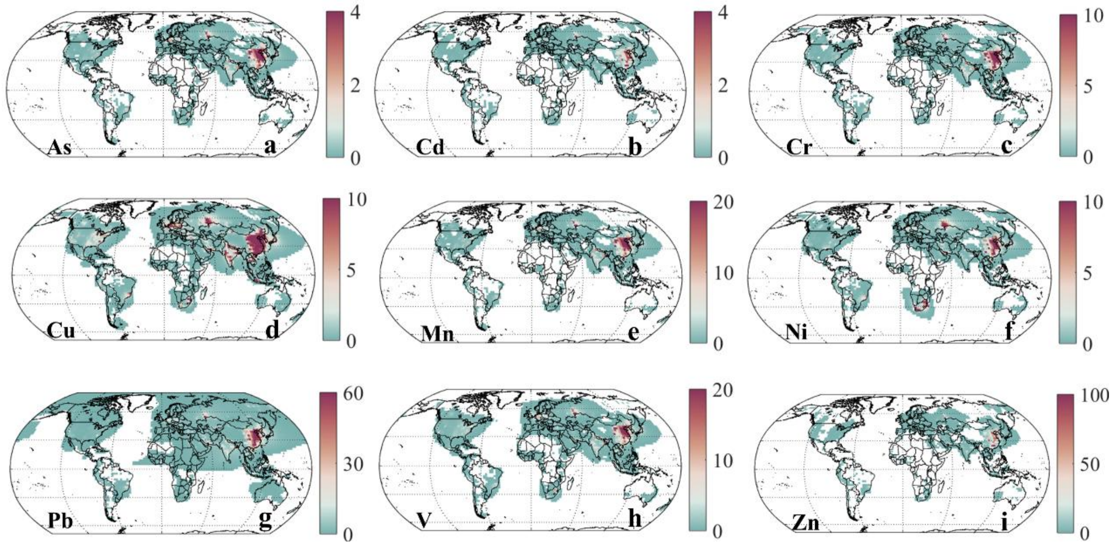

Figure S4 The global variations of ambient trace element concentrations (mean values) during January-April in 2020. The colorbar reflects the concentrations of trace elements.

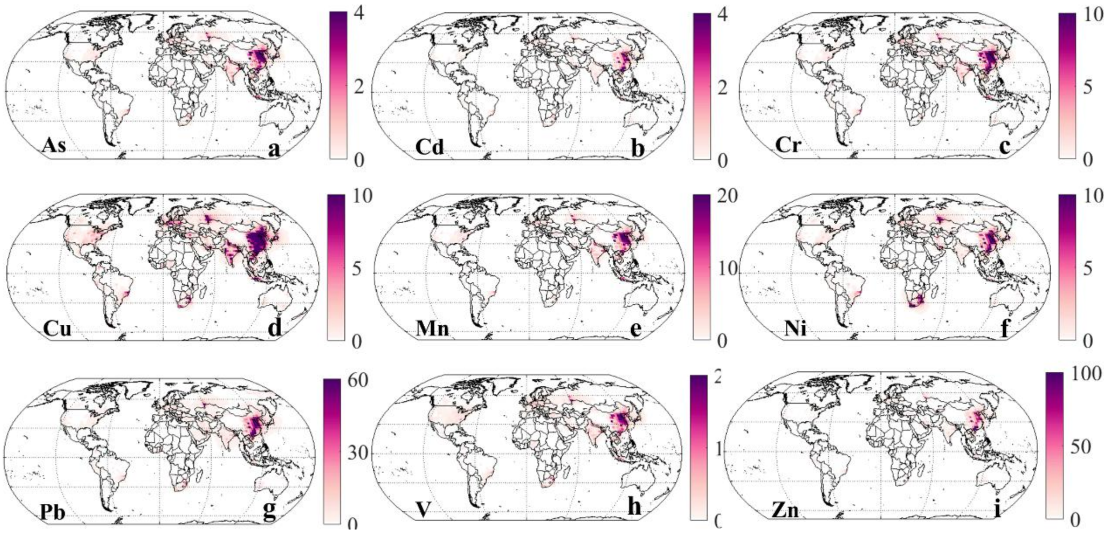

Figure S5 The violin graphs of nine trace elements including As (a), Cd (b), Cr (c), Cu (d), Mn (e), Ni (f), Pb (g), V (h), and Zn (i) in eight major regions during January-April in 2017-2019. Chi, Ind, WE, NA, SA, SS, Rus, and Aus represent China, India, West Europe, North America, South America, Sub-Sahara Africa, Russia, and Australia, respectively.

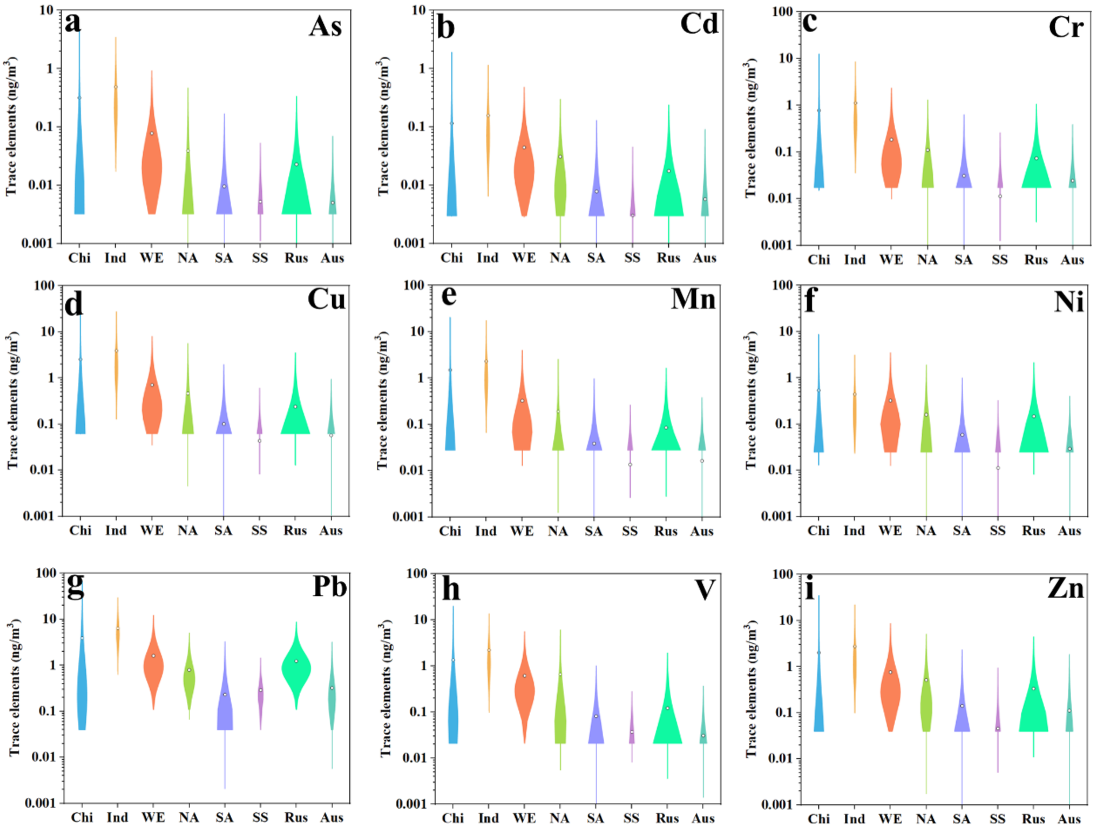

Figure S6 The emission and meteorological contributions to ambient Cd concentrations during 2017-2020 at global and eight major regions.

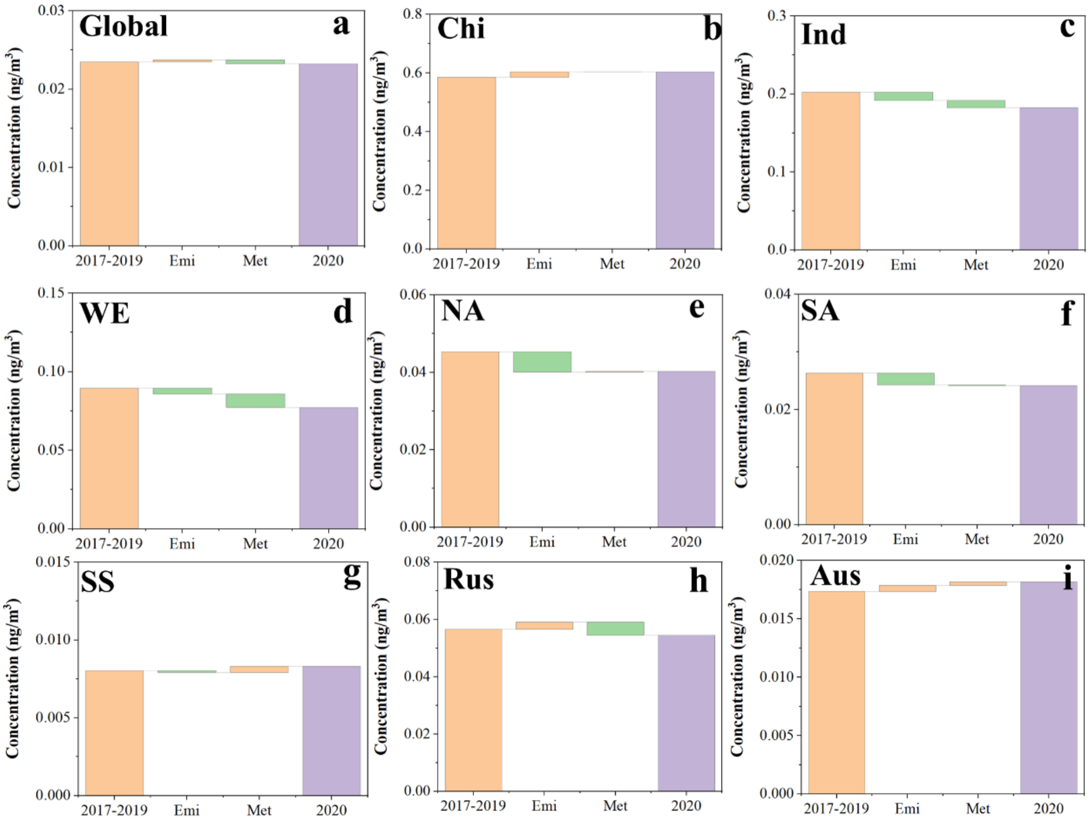

Figure S7 The emission and meteorological contributions to ambient Cr concentrations during 2017-2020 at global and eight major regions.

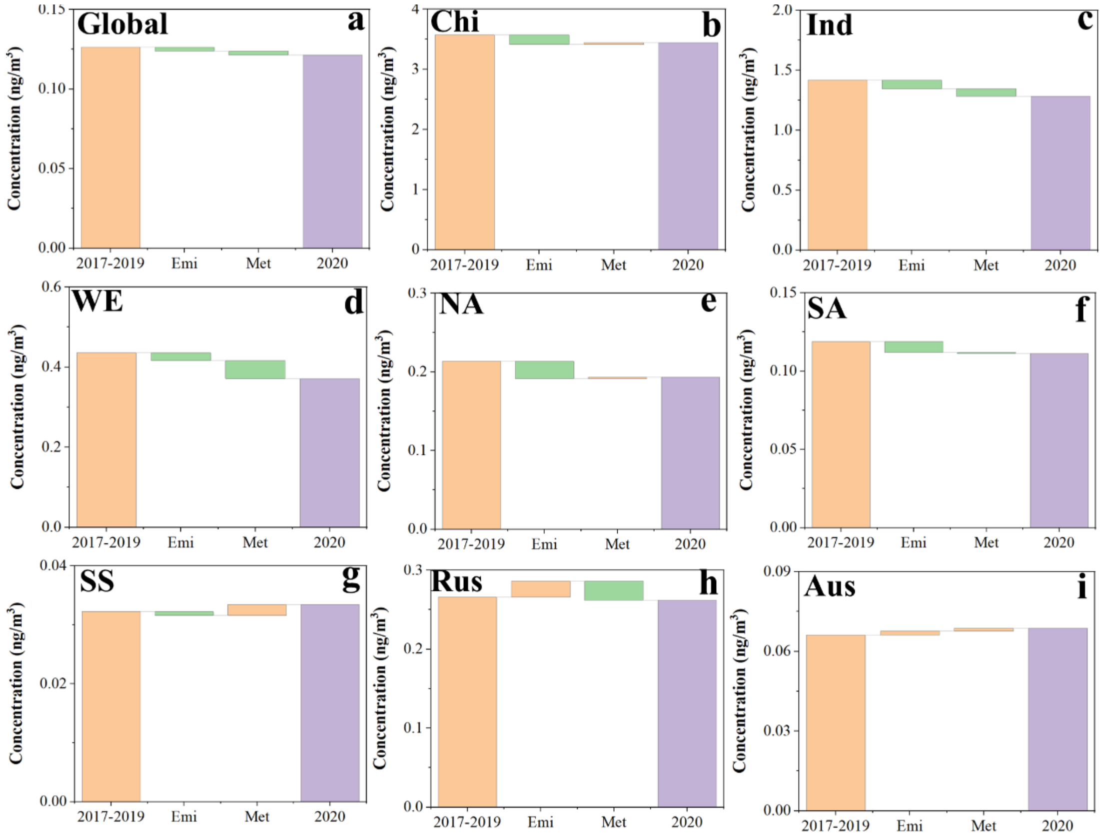

Figure S8 The emission and meteorological contributions to ambient Cu concentrations during 2019-2020 at global and eight major regions.

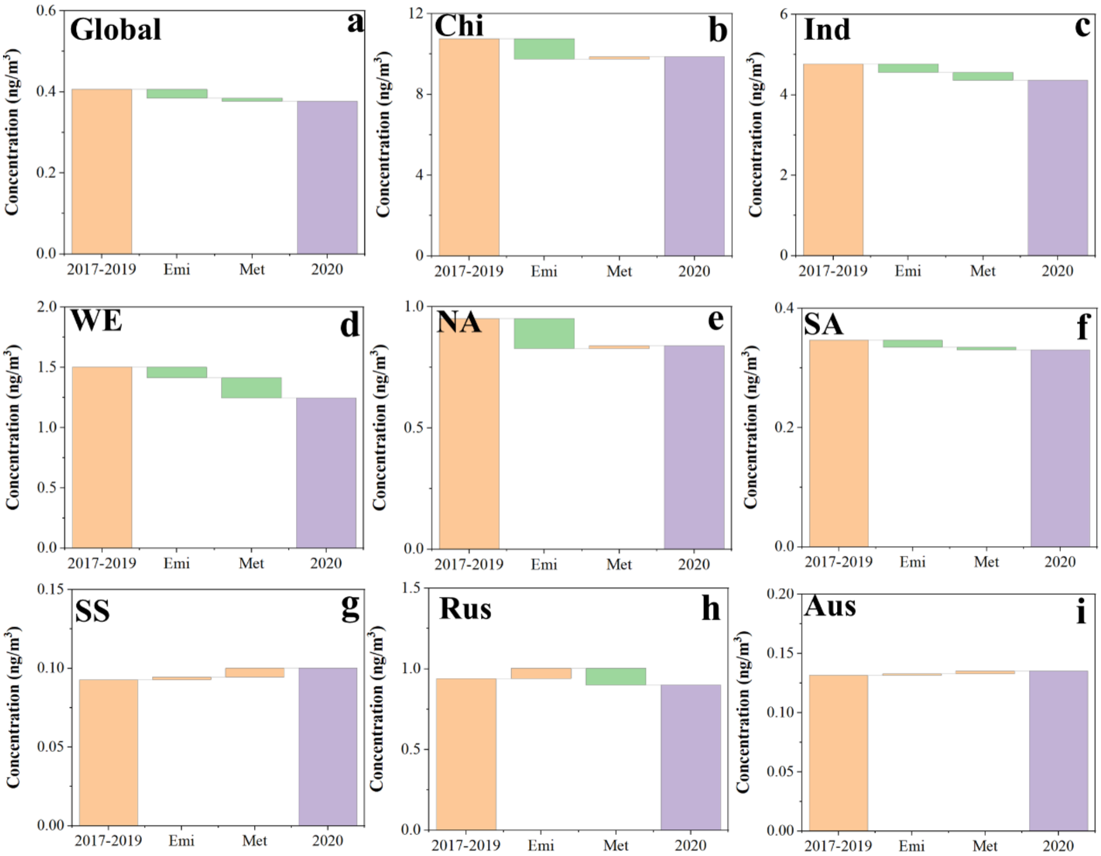

Figure S9 The emission and meteorological contributions to ambient Mn concentrations during 2019-2020 at global and eight major regions.

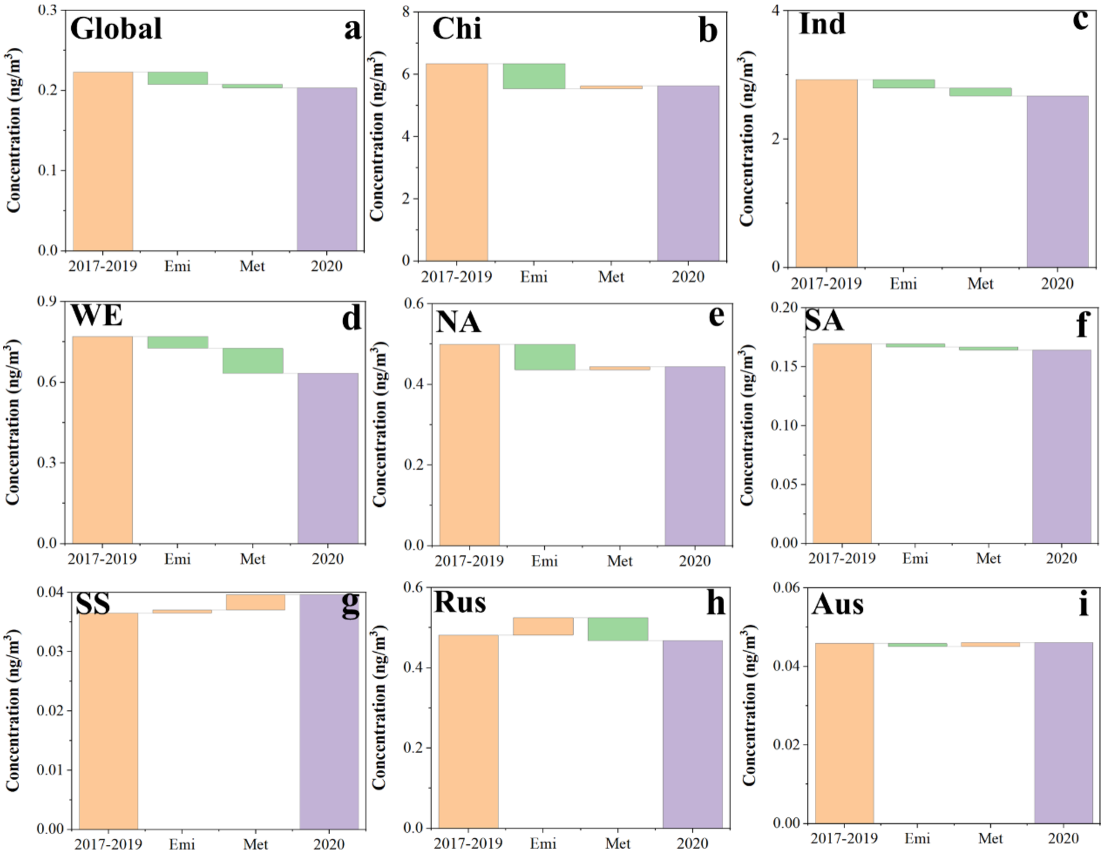

Figure S10 The emission and meteorological contributions to ambient Ni concentrations during 2019-2020 at global and eight major regions.

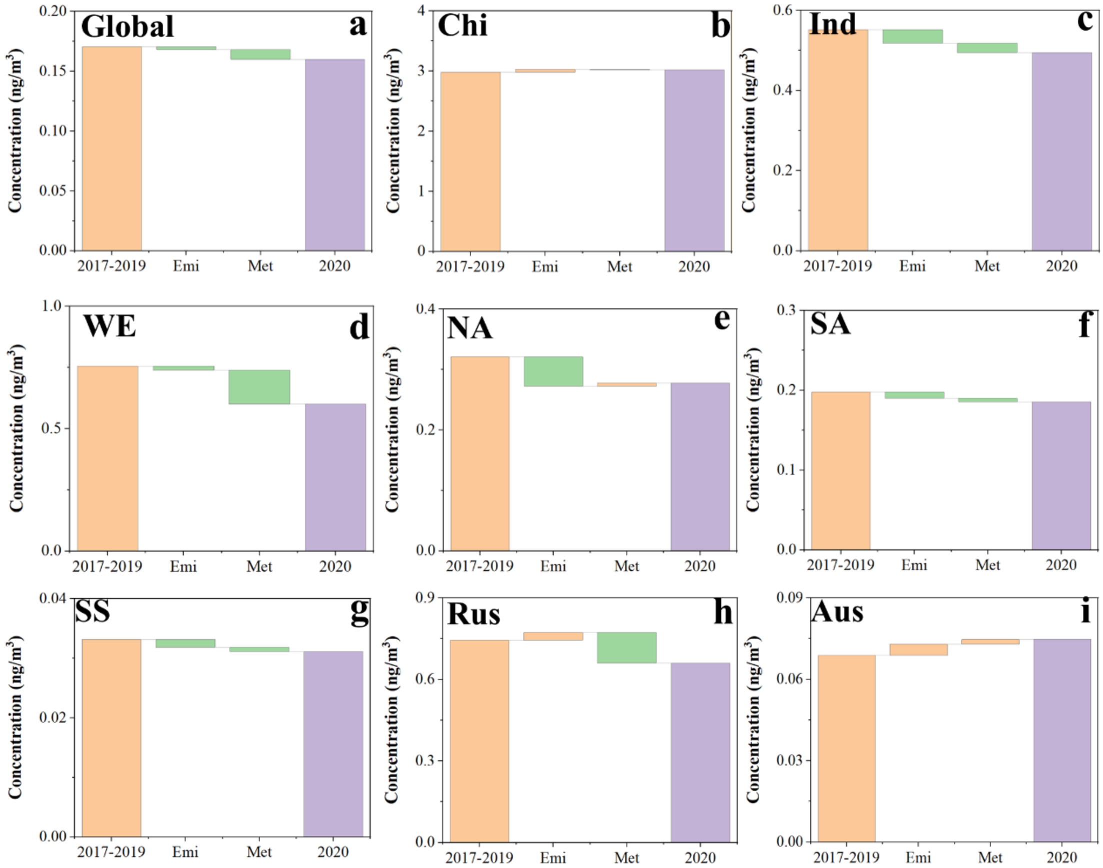

Figure S11 The emission and meteorological contributions to ambient Pb concentrations during 2019-2020 at global and eight major regions.

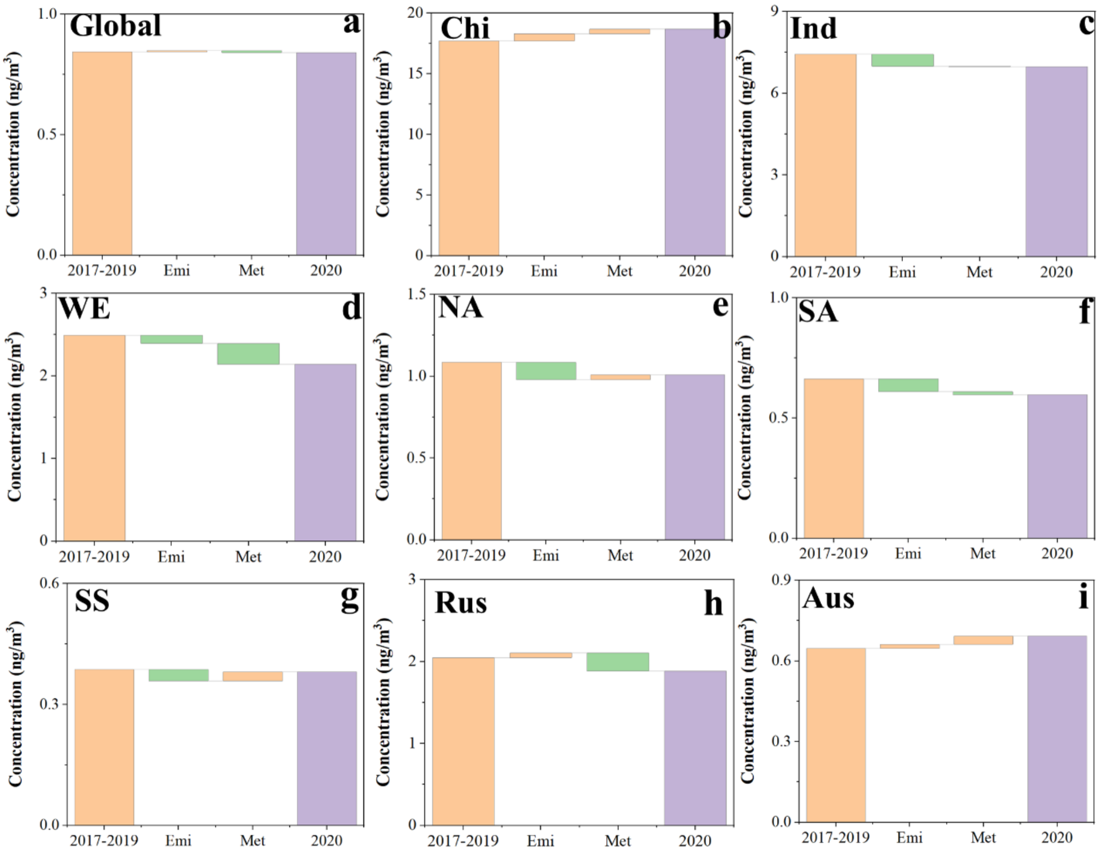

Figure S12 The emission and meteorological contributions to ambient V concentrations during 2019-2020 at global and eight major regions.

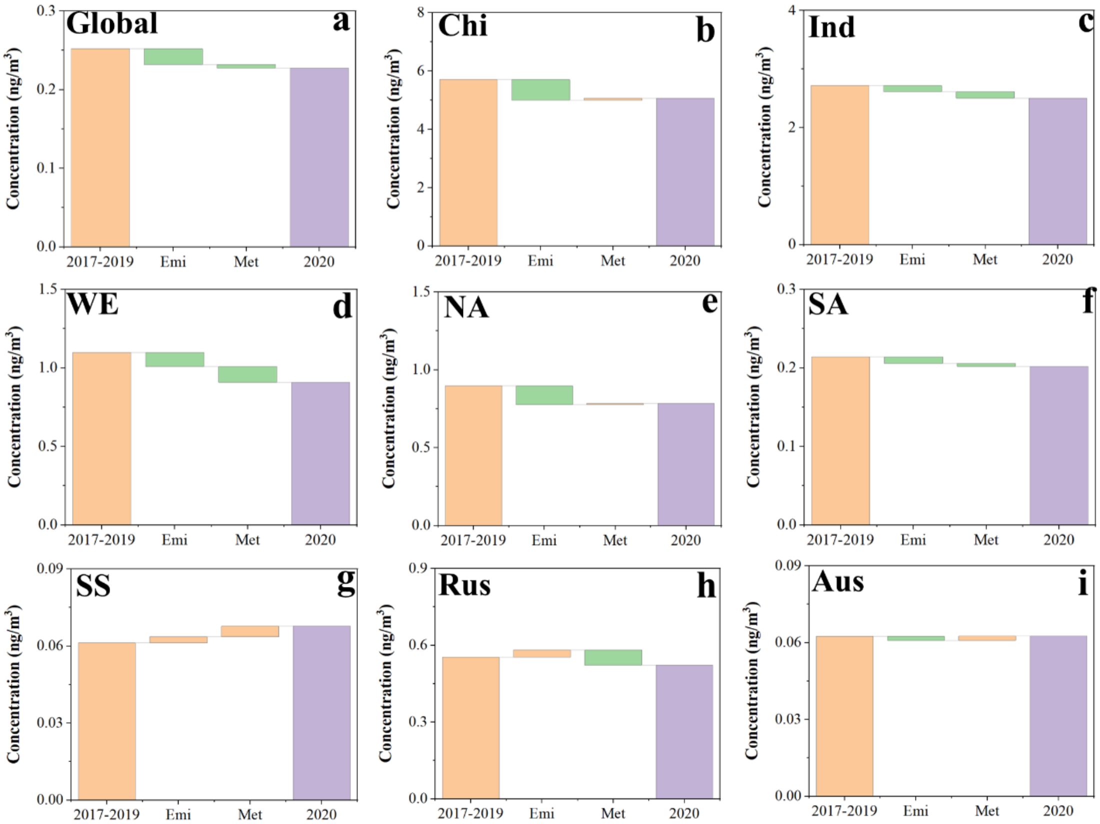

Figure S13 The emission and meteorological contributions to ambient Zn concentrations during 2019-2020 at global and eight major regions.

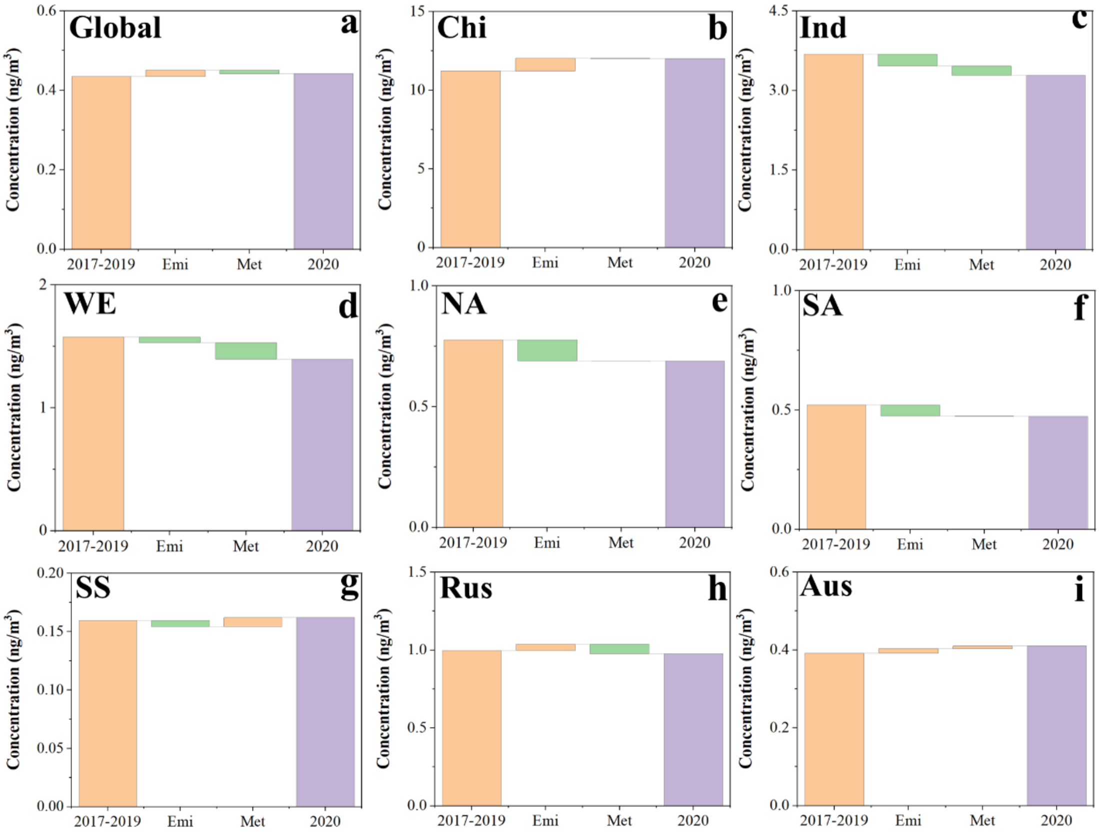

Figure S14 The anthropogenic and natural contributions to particle-bound As in eight major regions at the global scale before and during COVID-19 periods. Orange and blue colors represent anthropogenic and natural contributions.

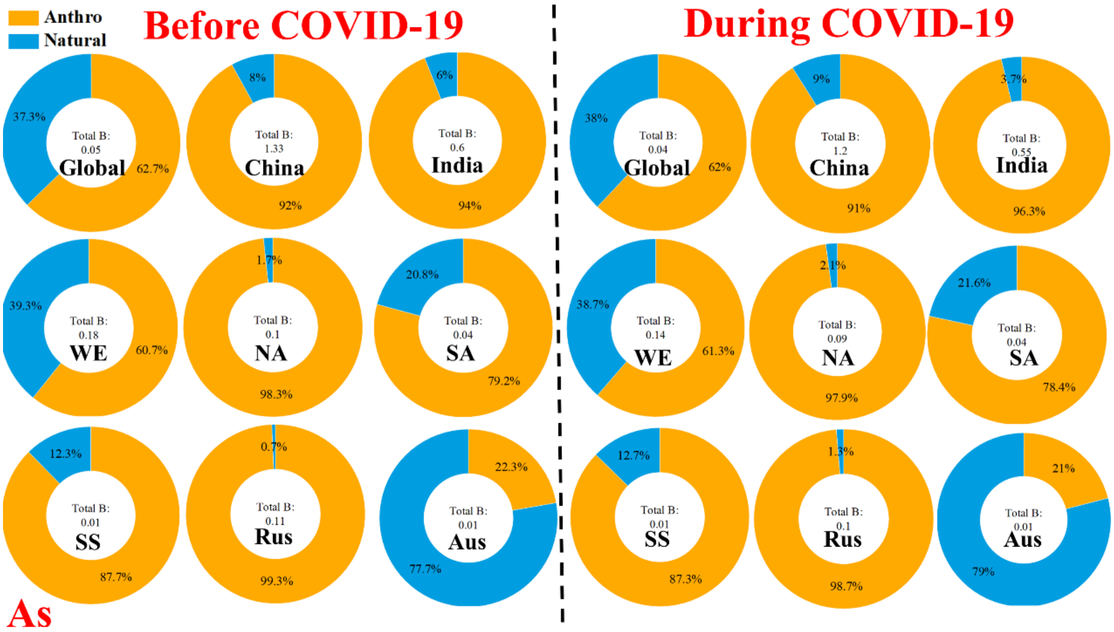

Figure S15 The anthropogenic and natural contributions to particle-bound Cd in eight major regions at the global scale before and during COVID-19 periods. Orange and blue colors represent anthropogenic and natural contributions.

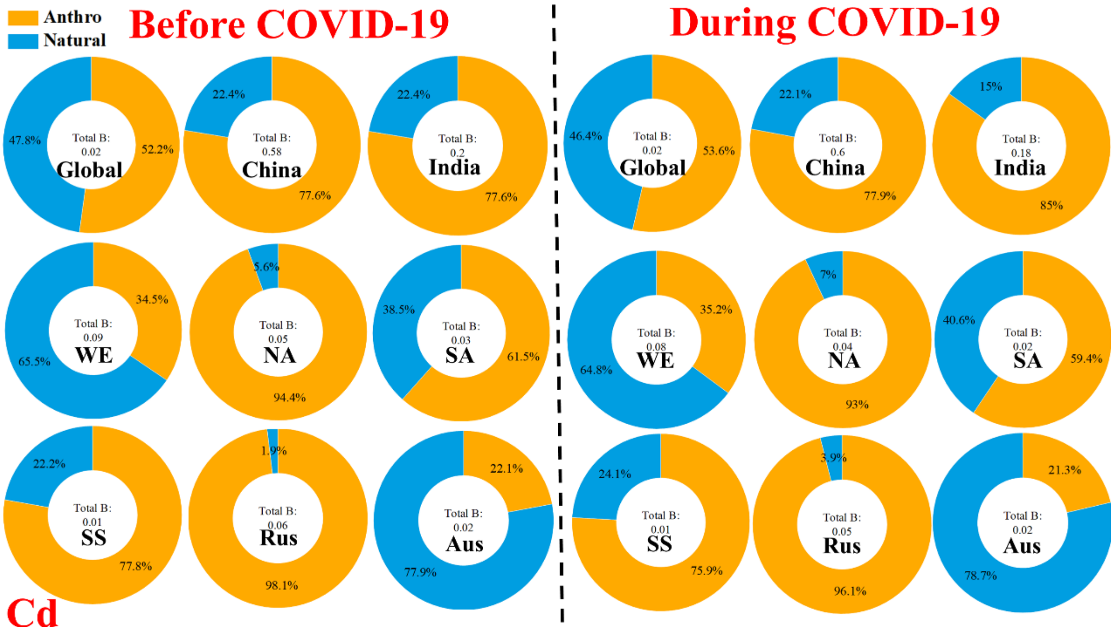

Figure S16 The anthropogenic and natural contributions to particle-bound Cr in eight major regions at the global scale before and during COVID-19 periods. Orange and blue colors represent anthropogenic and natural contributions.

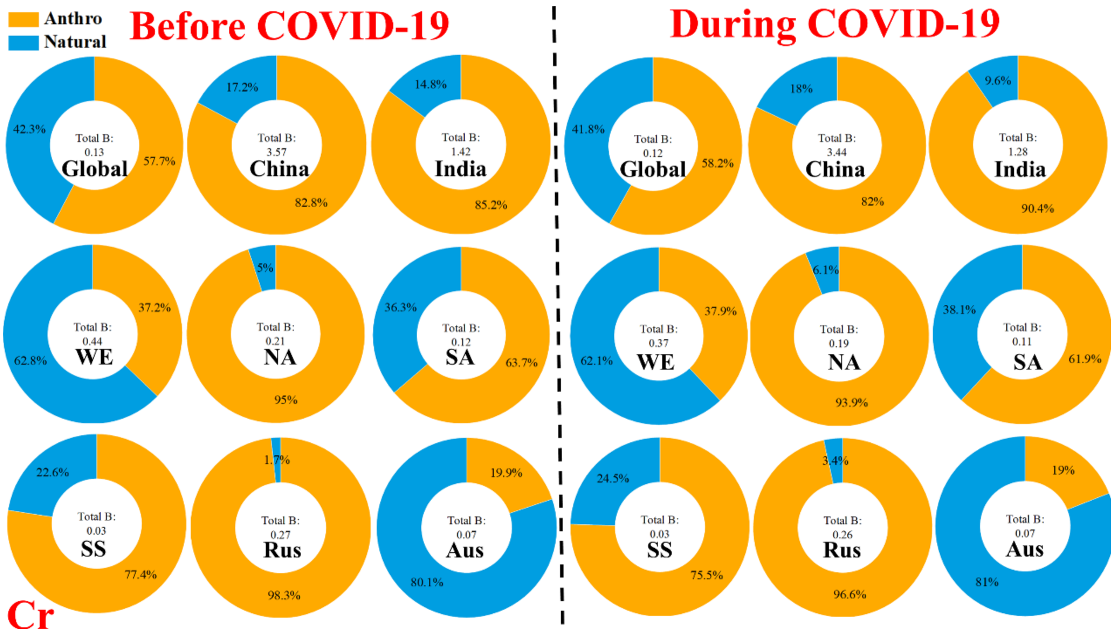

Figure S17 The anthropogenic and natural contributions to particle-bound Cu in eight major regions at the global scale before and during COVID-19 periods. Orange and blue colors represent anthropogenic and natural contributions.

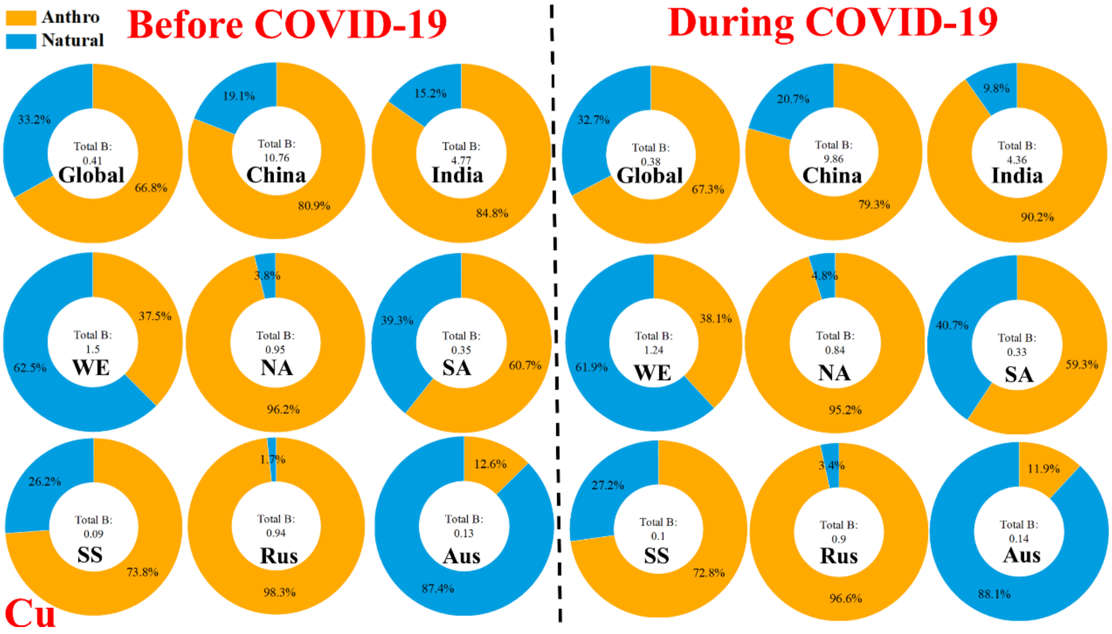

Figure S18 The anthropogenic and natural contributions to particle-bound Mn in eight major regions at the global scale before and during COVID-19 periods. Orange and blue colors represent anthropogenic and natural contributions.

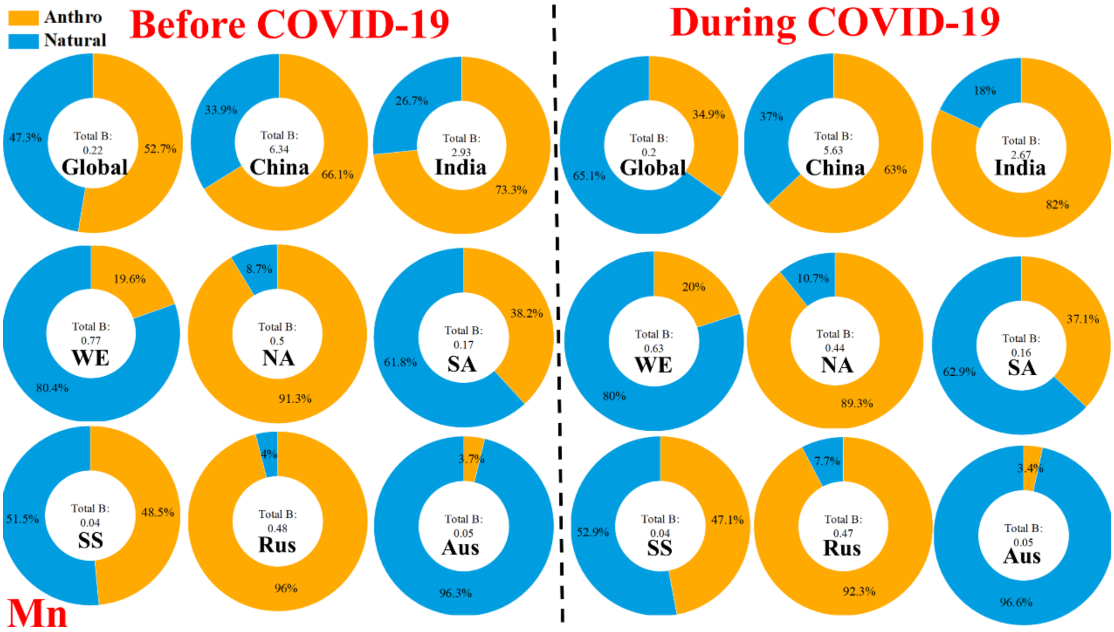

Figure S19 The anthropogenic and natural contributions to particle-bound Ni in eight major regions at the global scale before and during COVID-19 periods. Orange and blue colors represent anthropogenic and natural contributions.

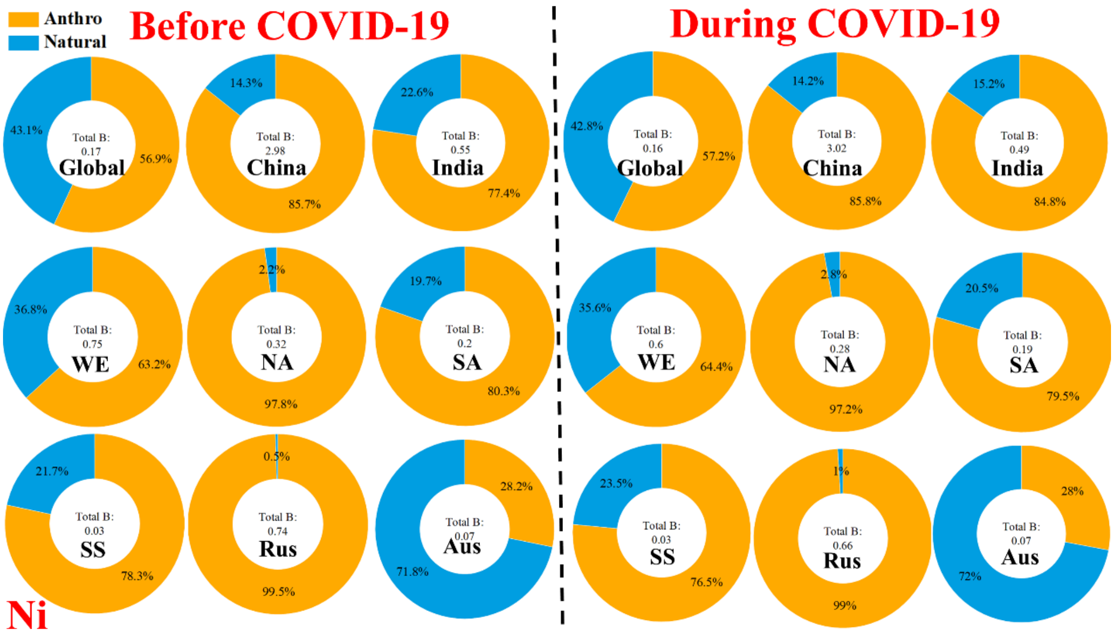

Figure S20 The anthropogenic and natural contributions to particle-bound Pb in eight major regions at the global scale before and during COVID-19 periods. Orange and blue colors represent anthropogenic and natural contributions.

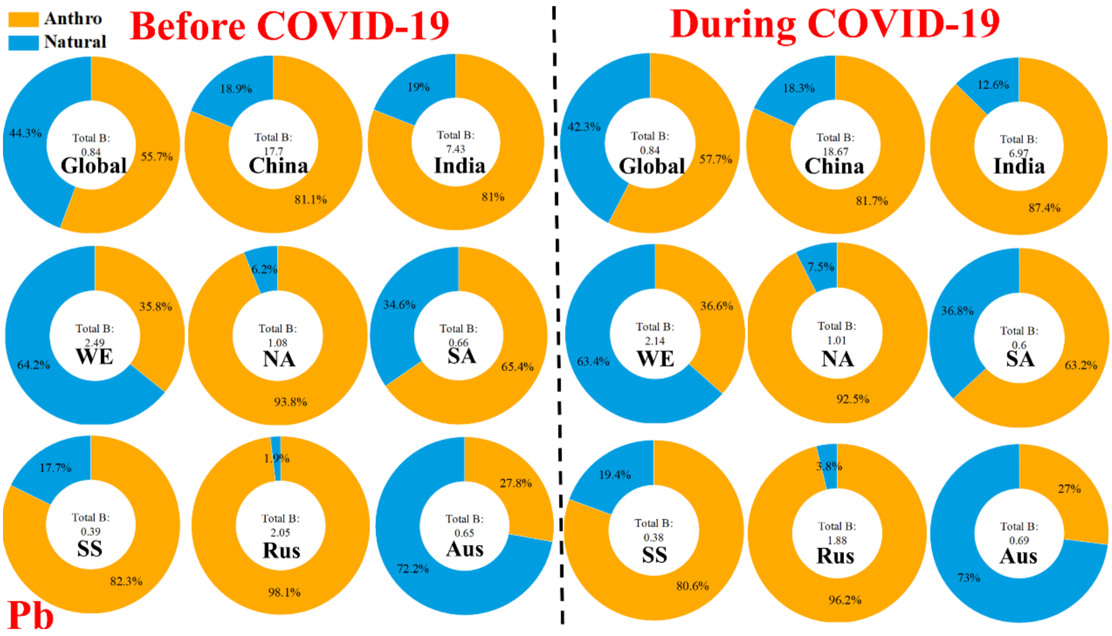

Figure S21 The anthropogenic and natural contributions to particle-bound V in eight major regions at the global scale before and during COVID-19 periods. Orange and blue colors represent anthropogenic and natural contributions.

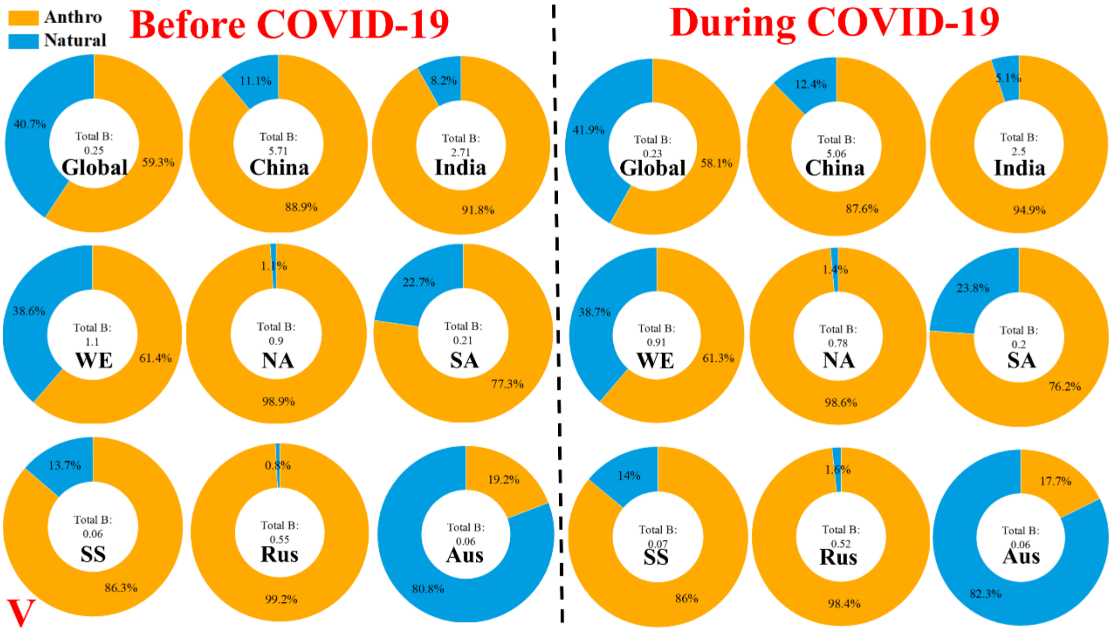

Figure S22 The anthropogenic and natural contributions to particle-bound Zn in eight major regions at the global scale before and during COVID-19 periods. Orange and blue colors represent anthropogenic and natural contributions.

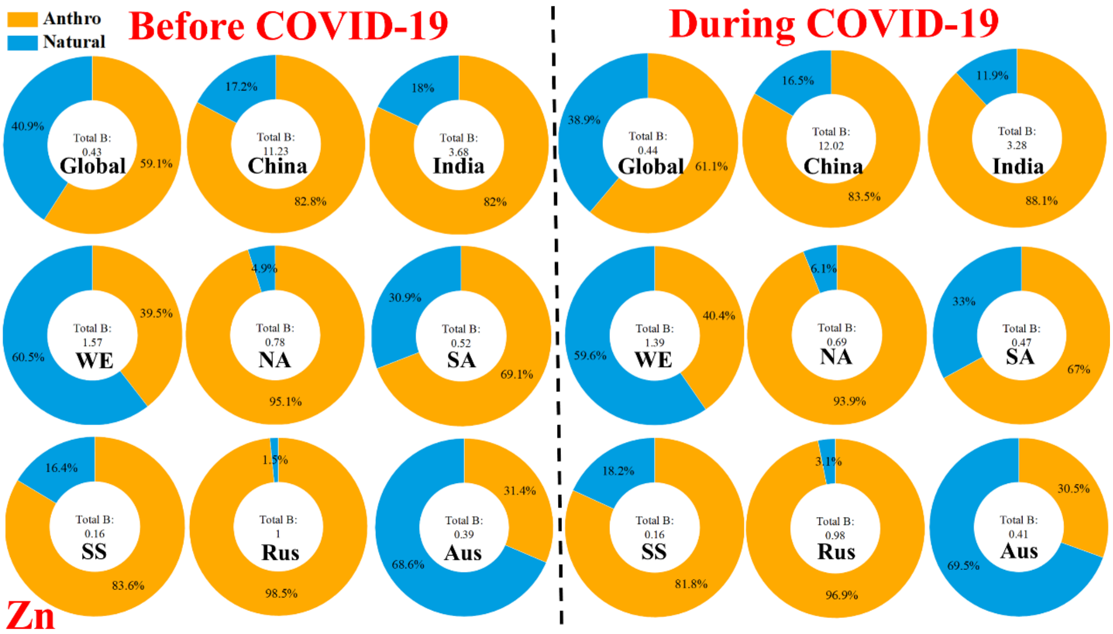

Figure S23 The ambient trace metal concentrations in major regions on the global scale in different emission scenarios. R, R_20%, R_40%, R_60%, and R_80% represent the global emission reduction ratios of 0% (base), 20%, 40%, 60%, and 80%, respectively.

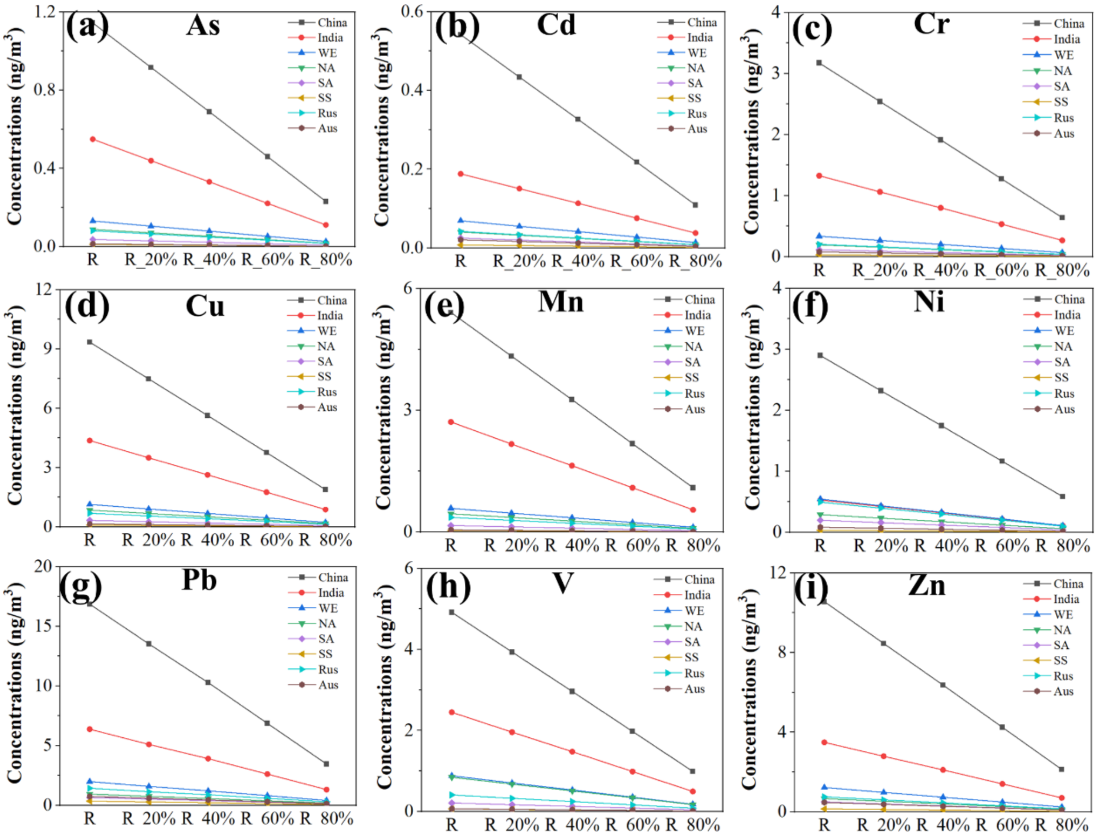

Figure S24 The total CR and HQ values of adults (a and c) and children (b and d) for all of the nine hazardous trace metals during January-April during 2017-2019.

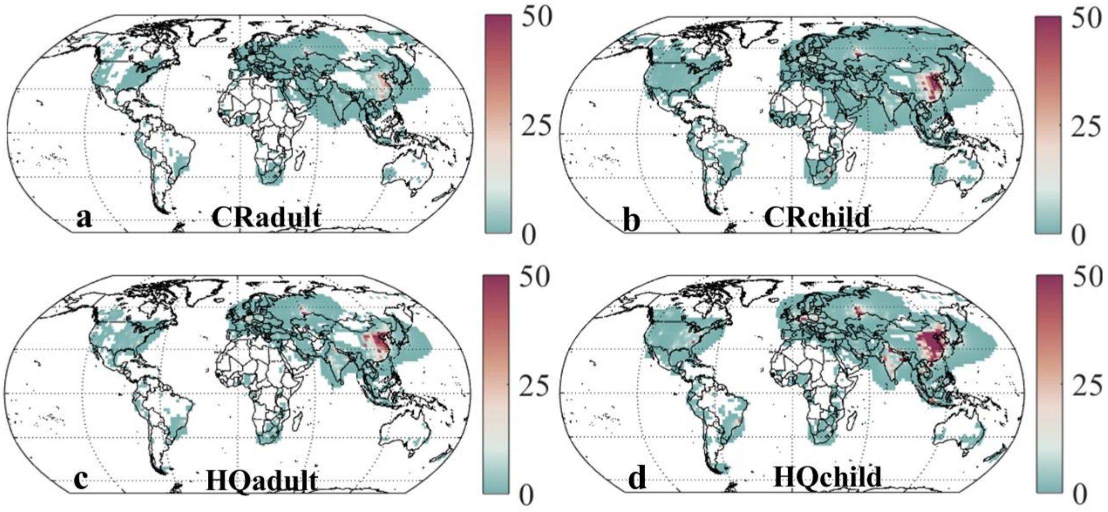

Figure S25 The total CR and HQ values of adults (a and c) and children (b and d) for all of the nine hazardous trace metals during January-April in 2020.

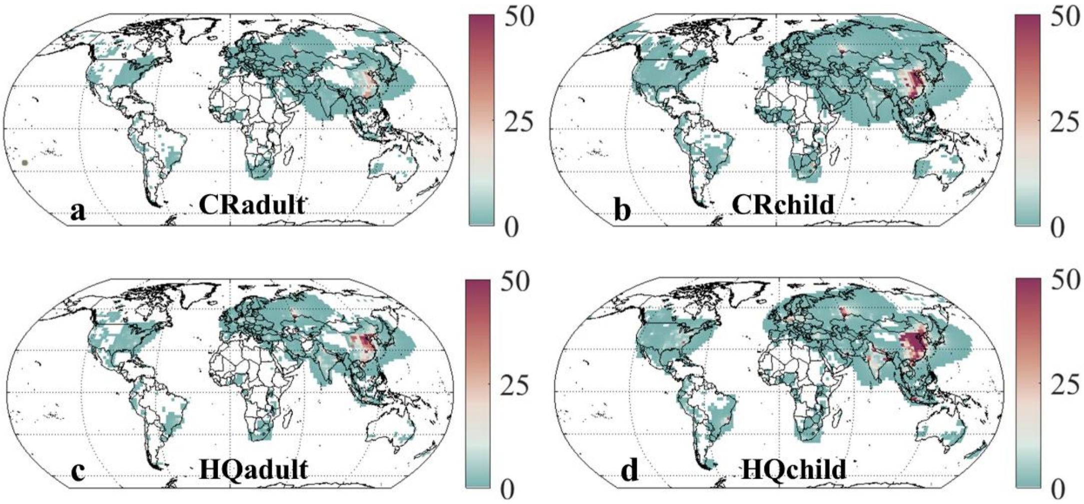

Figure S26 The sensitivity experiments of CR and HQ values to some indicators including InhR and BW. The x-axis and y-axis reflects the increase ratio of InhR/BW and the CR/HQ values, respectively.

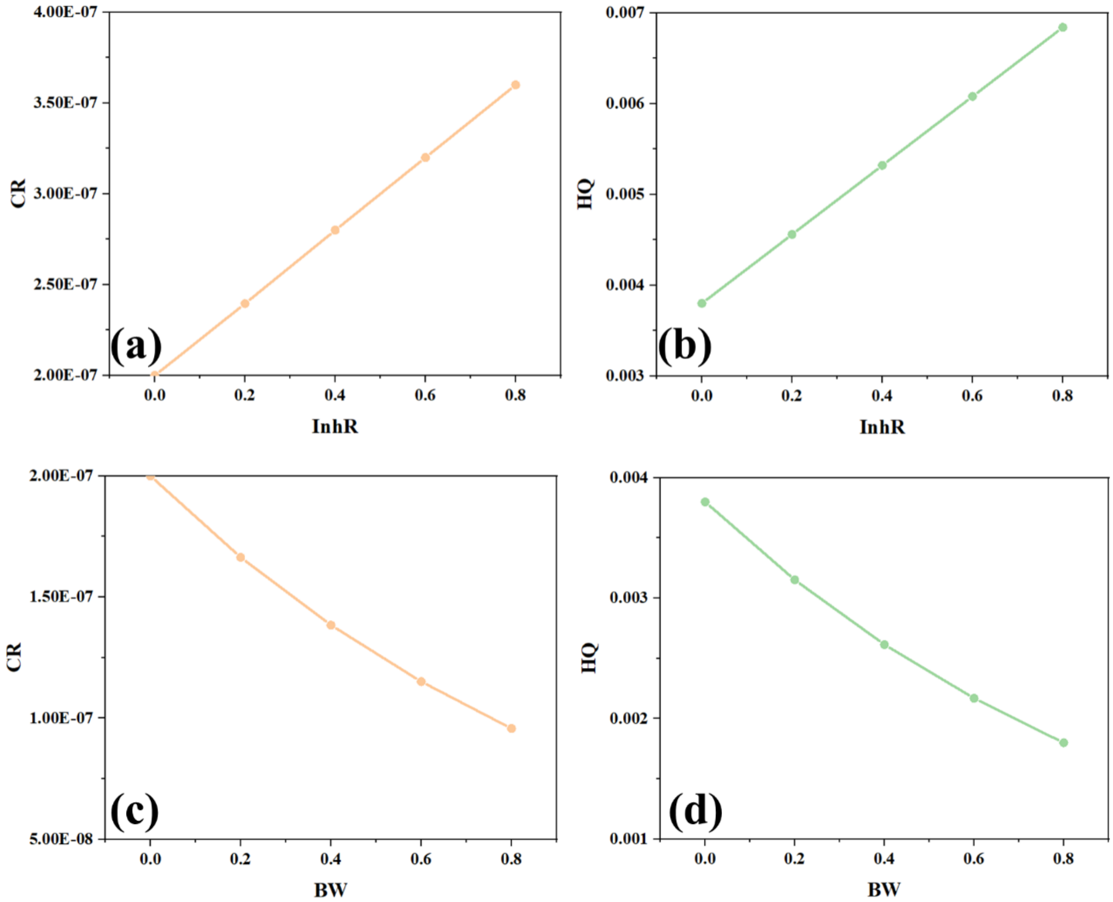

References

Báez, P., García, M., Torres, B.d.C., Padilla, H., Belmont, R., Amador, O., Villalobos-Pietrini, R. (2007) Origin of trace elements and inorganic ions in PM10 aerosols to the South of Mexico City. Atmospheric Research 85, 52-63.

Conway, T., Horner, T., Plancherel, Y., González, A. (2021) A decade of progress in understanding cycles of trace elements and their isotopes in the oceans. Chemical Geology 580, 120381.

Hu, C., Cheng, H., Li, J., Ke, H., Wu, W., Zhan, L., Wang, Z. (2018) Characteristics of elements and ecological risk assessment of heavy metals in PM10 and PM2. 5 in Huangshi. Environmental Chemistry 37, 138-145.

Jorquera, H., Barraza, F. (2013) Source apportionment of PM10 and PM2. 5 in a desert region in northern Chile. Science of the Total Environment 444, 327-335.

Lina, Y., Hao, Z., Juquan, Z., Zhenning, L., Shengrong, L. (2019) Comparative study on the distribution characteristics and sources of heavy metal elements in PM1, PM2. 5 and PM10 in Shijiazhuang City. Earth Science Frontiers 26, 263.

López, M.L., Ceppi, S., Palancar, G.G., Olcese, L.E., Tirao, G., Toselli, B.M. (2011) Elemental concentration and source identification of PM10 and PM2. 5 by SR-XRF in Córdoba City, Argentina. Atmospheric Environment 45, 5450-5457.

Olivelli, A., Arcucci, R., Rehkämper, M., van de Flierdt, T. (2025) Mapping the global distribution of lead and its isotopes in seawater with explainable machine learning. Earth System Science Data Discussions 2025, 1-36.

Salvador, P., Almeida, S., Cardoso, J., Almeida-Silva, M., Nunes, T., Cerqueira, M., Alves, C., Reis, M., Chaves, P., Artíñano, B. (2016) Composition and origin of PM10 in Cape Verde: Characterization of long-range transport episodes. Atmospheric Environment 127, 326-339.

Sohrin, Y., Bruland, K.W. (2011) Global status of trace elements in the ocean. TrAC Trends in Analytical Chemistry 30, 1291-1307.

Sun LongRen, S.L., Zheng ChunXia, Z.C., Wang WenQuan, W.W., Niu Ling, N.L. (2009) Concentration and enrichment characteristic of heavy metal elements in Urumqi atmospheric PM10.

Venter, A.D., Van Zyl, P.G., Beukes, J.P., Josipovic, M., Hendriks, J., Vakkari, V., Laakso, L. (2017) Atmospheric trace metals measured at a regional background site (Welgegund) in South Africa. Atmospheric Chemistry and Physics 17, 4251-4263.

Wang, J., Wang, C., Chen, Z.-L. (2011) Heavy Metal Pollution of PM (10)/PM (2. 5) Near-surface in Guiyang. Huanjing Kexue yu Jishu 34.

Wu, X., Chen, B., Wen, T., Shahid, I., Habib, A., Shi, G. (2019) Comparison of Concentrations and Chemical Compositions of PM10 during Hazy and Non-Hazy Days in Beijing and Islamabad. J. Shandong Univ.(Natural Science) 54, 42-49.

YU YJ, Y.L. (2013) Health risk assessments of heavy metals and PAHs bound to PM 10 in Lanzhou city. Acta Sci Circumst 33, 2919-2927.